

# Bacteria Adherence Properties of Nitrogen-Doped TiO<sub>2</sub> Coatings by Plasma Surface Alloying Technique

WANG Hefeng<sup>1,2</sup>, TANG Bin<sup>2</sup>, LIN Naiming<sup>2</sup>, LI Xiuyan<sup>2</sup>, FAN Ailan<sup>2</sup>, SHU Xuefeng<sup>1,\*</sup>

(1. Institute of Applied Mechanics and Biomedical Engineering, Taiyuan University of Technology, Taiyuan 030024, China; 2. Research Institute of Surface Engineering, Taiyuan University of Technology, Taiyuan 030024, China)

**Abstract:** In order to obtain a high-performance surface on 316L stainless steel (S. S) that can meet the requirements in medical material field environment, nitrogen-doped titanium dioxide (TiO<sub>2-x</sub>N<sub>x</sub>) was synthesized by oxidative annealing the resulted TiN<sub>x</sub> coatings in air. Titanium nitride coatings on 316L S. S were obtained by plasma surface alloying technique. The as-prepared coatings were characterized by X-ray diffraction, glow discharge optical emission spectrometer (GDOES), scanning electron microscopy and X-ray photoelectron spectroscopy, respectively. The bacteria adherence property of the TiO<sub>2-x</sub>N<sub>x</sub> coatings on S. S on the oral bacteria *Streptococcus Mutans* was investigated and compared with that of S. S by fluorescence microscopy. The mechanism of the bacteria adherence was discussed. The results show that the TiO<sub>2-x</sub>N<sub>x</sub> coatings are composed of anatase crystalline structure. SEM measurement indicates a rough surface morphology with three-dimensional homogenous protuberances after annealing treatment. Because of the photocatalysis and positive adhesion free energy, the TiO<sub>2-x</sub>N<sub>x</sub> coatings inhibit the bacteria adherence.

**Key words:** titanium dioxide; plasma alloying; stainless steel; bacteria adherence

## 1 Introduction

AISI 316L austenitic S. S is a technologically important material, which has been widely used in various sectors of industry due to its excellent corrosion resistance in a variety of engineering environments<sup>[1,2]</sup>. It has also been found to have applications in the biomedical sectors for the fabrication of medical devices and body implants owing to its good corrosion resistance and biocompatibility<sup>[3,4]</sup>. However, bacterial infection after implant placement is a significant rising complication. The bacteria adherence is the first-line factor that leads to infections. It is crucial to improve the antibacterial adherence property of S. S. Titanium nitride coatings have become universally accepted coatings due to their mechanical properties, such as hardness and wear resistance and biocompatibility.

The major applications of the coatings are protective coatings on steels, diffusion barriers in integrated circuit industry, and decorative coatings. Recently, it has been reported that TiN oxidation is one way to synthesize nitrogen-doped TiO<sub>2</sub>. Morikawa *et al* synthesized N-doped rutile TiO<sub>2</sub> by oxidation of TiN<sup>[5]</sup>. Cui *et al* also reported the synthesis of Nitrogen-doped titanium dioxide by oxidative annealing the resulted TiN thin film in air<sup>[6]</sup>, but they did not study its antibacterial adherence properties applied to S. S.

The plasma surface alloying technique is a very promising surface engineering technique<sup>[7]</sup>. Its greatest advantage lies in no element mutation between surface alloying layer and substrate interface. The surface alloying layers are duplex layers, composed of diffusion layer and surface coatings. The component of elements in the diffusing layer changes gradually which can enhance the load-bearing capacity to the coatings and ensure the durability of the coatings.

In principle, N-doped TiO<sub>2</sub> coatings could be obtained on metal substrate with Ti target in Ar/O<sub>2</sub>/N<sub>2</sub>, but two technologically important questions arise: i) Oxygen would lead to "target poisoning", which will affect the stability of process parameters and the deposition rate and ii) In glow discharge sputtering, the temperature of the substrate is higher than 800 °C.

©Wuhan University of Technology and SpringerVerlag Berlin Heidelberg 2012

(Received: May 19, 2011; Accepted: Jan. 9, 2012)

WANG Hefeng (王鹤峰): Ph D candidate; E-mail: whfytut@163.com

\*Corresponding author: SHU Xuefeng (树学峰): Prof.; Ph D; E-mail: shuxf@tyut.edu.cn

Funded by the National Natural Science Foundation of China (Nos.11172195, 51171125), International Cooperative Scientific Project of Shanxi Province (No.2010081016), and Science and Technology Committee of Shanxi Province (No.20110321051)

Experiment results show that rutile TiO<sub>2</sub> coatings will be formed on the substrate at this temperature, rather than the anatase TiO<sub>2</sub> coatings with good photocatalytic properties.

Based on these analyses, the N-doped TiO<sub>2</sub> coatings were prepared by two steps. Firstly, the TiN<sub>x</sub> coatings were deposited by plasma surface alloying technique. All the resulted TiN<sub>x</sub> coatings were subsequently annealed in air at 450 °C for 2 h to oxidize. The antibacterial adherence properties of the N-doped TiO<sub>2</sub> coatings in AISI316L on the oral bacteria *Streptococcus Mutans* was investigated and compared with that of AISI316L S. S.

## 2 Experimental

### 2.1 Sample preparation

The 316L S. S samples (Φ20 mm×5 mm) were grounded with No. 80-1500 emery papers, and then polished with 0.3 and 0.05 μm alumina powder. Finally, the surfaces of samples were cleaned by ethanol and acetone.

The N-doped TiO<sub>2</sub> coatings were prepared by two steps. Firstly, the TiN<sub>x</sub> coatings were deposited by plasma surface alloying technique (double glow LS-750 plasma alloying equipment) using 99.99% Ti as target in the Ar/N<sub>2</sub>. The principle of double glow discharge is employed to ionize argon ions bombarding the source electrode and sputtering titanium ions, atoms or particles, which deposit on S. S surface and diffuse into the specimen at a high temperature, obtaining a gradient alloying layer on S. S surface<sup>[8]</sup>. The process parameters were as follows: the Ar/N<sub>2</sub> mixture gas pressure was 30-40 Pa (N<sub>2</sub>:Ar = 1:2), the source voltage for supplying Ti elements was -1 100 to -1 150 V, the cathode (specimen) voltage was -500 to -550 V, the distance from the source target to the substrate sample was 15 mm, the process temperature was 950 °C and the process duration was 3 h. All the resulted TiN<sub>x</sub> coatings were subsequently annealed in air at 450 °C for 2 h to oxidize and crystallize the samples.

### 2.2 Characterization

The crystal structure of the as-prepared samples was analyzed by D/max 2500 X-ray diffraction (XRD) with the 1.54 Å Cu Kα line as the excitation source. Chemical states of the coatings were obtained by X-ray photoelectron spectroscopy (XPS) using ESCALAB 250 spectrometer with Al Kα as the radiation source. The binding energies obtained in XPS analysis were corrected by referencing the C1s line to 284.6 eV.

The component distribution of the elements across the coatings was analyzed using GDA750 glow-discharge optical emission spectroscopy (GDOES). Surface morphology was studied by scanning electron microscope (SEM). The surface roughness (*Ra*) of the N-doped TiO<sub>2</sub> coatings and S. S substrate were investigated by TR 240 rough-meter.

### 2.3 Bacteria adherence

The bacteria adherence properties of the N-doped TiO<sub>2</sub> coatings on S. S and S. S substrate were tested using *Streptococcus Mutans* strain ATCC#25175. Bacteria were pre-cultured in nutrient broth at 37 °C for 24 h, and then the Tris-HCl suspension was diluted to approximately 1.5×10<sup>7</sup> bacteria per mL with sterilized distilled water. S. S substrate and surface modified specimens were put into sterilized glass bottles with 5 mL of bacterial suspension and were incubated at 37 °C for 1 h. After incubation, the samples were rinsed with distilled water six times, fixed in 3% glutaraldehyde at 4 °C for 30 min and stained with a 1% Acridine Orange solution for 30 min. Bacteria number and bacteria morphology on each sample were analyzed using a fluorescence microscope (OLYMPUS-BX51T-32000) at 400× magnification.

### 2.4 Antibacterial test

The antibacterial activity of the coatings obtained against *S.aureus* was studied using the antibacterial drop-test. Microorganisms were cultured on the culture medium at 37 °C for 24 h. Cultured bacteria were added in 10 mL saline solution to reach approximately the concentration of bacteria corresponding to 10<sup>8</sup> colony forming units per milliliter (CFU/mL). A portion of the saline solution containing the bacteria was diluted to 10<sup>6</sup> CFU/mL for the drop-method antibacterial experiments. An N-TiO<sub>2</sub> coated S. S sample and an untreated SS Sample were used as blanks. The samples were placed into sterilized 80 mm Petri dishes. Then 100 μL saline solutions with *S.aureus* at a concentration of 10<sup>6</sup> CFU/mL were added onto the surface of each specimen. The samples were illuminated with a fluorescent lamp (80 W) at room temperature and cultured for 4 hours. The lamp was perpendicular to the surface at a distance of 50 cm. After time period, the bacteria containing drops were washed from the sample surface using 5 mL saline solution in the sterilized Petri dishes. Then 10 μL of each bacteria suspension was dispersed on the Brain Heart Infusion Agar medium and incubated for 24 h at 37 °C. The numbers of surviving bacteria on the mediums were counted after incubation.

### 3 Results and discussion

#### 3.1 Structural characterization

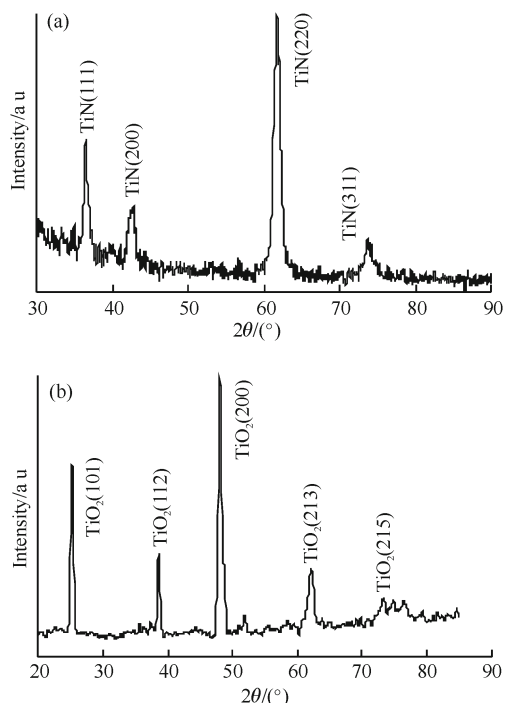


Fig.1 XRD patterns for TiN samples deposited (a) before and (b) after annealing

There are two distinct steps in the experimental preparation of nitrogen-doped  $\text{TiO}_2$  coatings. Initially, TiN coatings were deposited on the surface of S. S substrate. The second stage of the preparation process was a simple conversion of the resulted TiN coatings to the oxide by heat treatment in air. The oxidation was performed at  $450^\circ\text{C}$  in an attempt to produce anatase  $\text{TiO}_2$ . Fig.1 shows the XRD patterns of the TiN coatings deposited on S. S (a) and after annealing (b). It can be seen from Fig.1 (a) that the as-deposited coatings sputtered under Ar and  $\text{N}_2$  mixture are composed of TiN. The sample is of homogeneous anatase phase after annealing and no specific peaks of TiN are detected, which indicates that the  $\text{TiN}_x$

coatings have been converted into  $\text{TiO}_2$  after annealing at  $450^\circ\text{C}$  in air for 2 h. The anatase phase of  $\text{TiO}_2$  coatings is usually formed at about  $300^\circ\text{C}$  calcination temperature. In our experiment, N-doped  $\text{TiO}_2$  coatings are anatase structure at  $450^\circ\text{C}$ . These results suggest that the doped-N particles in the  $\text{TiO}_2$  coatings hinder to form the anatase phase. As for the N-doped  $\text{TiO}_2$  coated sample, there appear a series of peaks located at 25.20, 38.60, 48.05, 62.1 and 74.8. The XRD peaks of the N-doped samples have obvious shift toward lower or higher angular side compared with standard peaks of anatase titanium dioxide (JCPDS: 84-1285). This may be due to the effect of N-doping.

The XPS spectra of N- $\text{TiO}_2$  coatings deposited are shown in Fig.2 for N 1s, Ti 2p and O 1s peaks. Fig.2(a) shows the chemical binding state of N 1s of the sample. The peak is observed at 399.9 eV. Dong *et al*<sup>[9]</sup> observed three peaks of N 1s at 397.8, 399.9 and 401.9 eV and has attributed to N-Ti-N, O-Ti-N and Ti-N-O linkage respectively. Sakthivel *et al*<sup>[10]</sup> observed an intense peak at 400.1 eV that was assigned to hyponitrite species and concluded that the higher binding energy is due to the lower valence state of N in N doped  $\text{TiO}_2$ . Many researches pointed out that intense peak at 400 eV are due to oxidized nitrogen like Ti-O-N or Ti-N-O linkages. Recently, Gopinath observed N 1s binding energy at 401.3 eV and claimed the presence of Ti-N-O linkage on the surface of N doped  $\text{TiO}_2$  nano particles<sup>[11]</sup>. The peak at 399.9 eV is ascribed to O-Ti-N, Ti-N-O linkages in the  $\text{TiO}_2$  lattice.

Fig.2(b) presents that Ti 2p peaks appear at 458.0 eV and 463.6 eV after heat treatment respectively which are attributed to O-Ti-O linkages in  $\text{TiO}_2$ .

Fig.2(c) shows that O 1s peaks appear at 529.3 eV and 531.5 eV, respectively. The O 1s peak at 529.3 eV is assigned to the lattice oxygen atom of  $\text{TiO}_2$ , and the peak at 531.5 eV is closely related to the hydroxyl groups (-OH) resulting mainly from chemisorbed water. The increase in surface hydroxyl content is advantageous for trapping more photogenerated holes

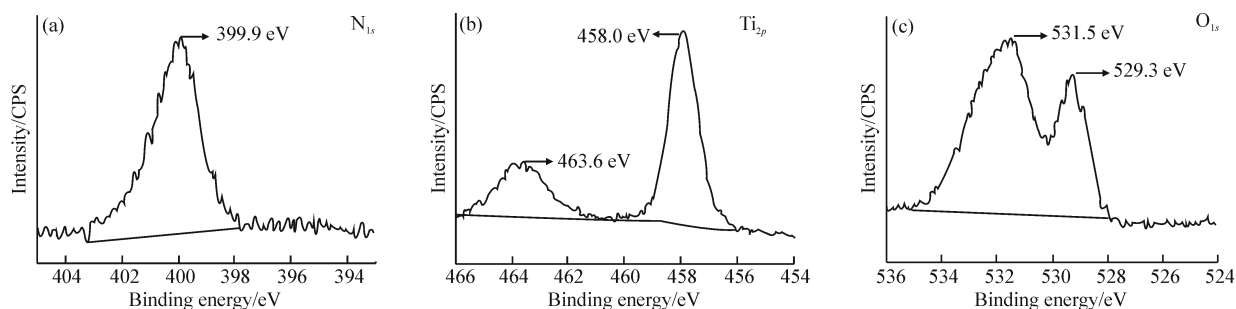


Fig.2 X-ray photoelectron spectral details collected from N-doped  $\text{TiO}_2$  sample deposited: (a) N 1s; (b) Ti 2p; and (c) O 1s peaks

and thus preventing electron-hole recombination<sup>[8]</sup>.

Fig.3 shows the SEM image for the resulted N-doped sample. Many three-dimensional homogenous protuberances can be seen for the doped TiO<sub>2</sub> coatings, but no cracks or pinholes in the coatings. It is noted that the N-doped TiO<sub>2</sub> coatings have entirely shielded the S. S substrate.

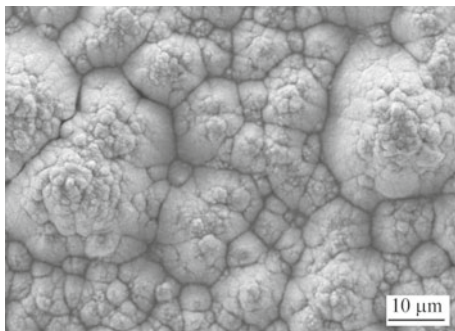


Fig. 3 SEM image for N-doped TiO<sub>2</sub> sample

Meantime, the surface roughness of the coatings was also measured by rough-meter. The average roughness of N-doped TiO<sub>2</sub> coatings is  $0.20 \pm 0.01 \mu\text{m}$ , which is much higher than the roughness of substrate ( $0.08 \pm 0.01 \mu\text{m}$ ).

Fig.4 demonstrates that some gradient

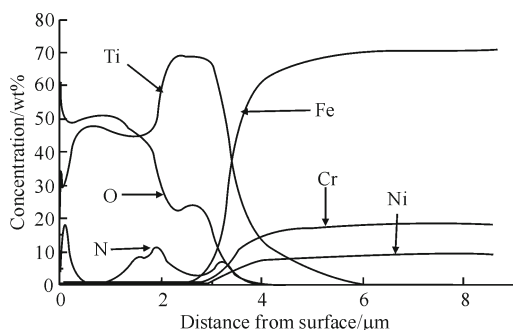


Fig. 4 Component distribution of N-doped TiO<sub>2</sub> modified layer

distributions of Ti, N, O and Fe, Cr, Ni elements exist in the Ti-N-O coatings. After thermal oxidation treatment, Ti-N-O coatings are composed of deposition and diffusion layer. The layer reaches a thickness of approximately  $4.5 \mu\text{m}$ . In internal diffusion region, mutual diffusion of Ti and substrate alloy elements occur, causing the mixing of the elements at the interface, which can significantly improve bonding strength of doped TiO<sub>2</sub> coatings with S. S substrate.

### 3.2 Bacteria adherence property

In order to clarify the antibacterial adherence properties for the preparation N-doped TiO<sub>2</sub> coatings under illumination of Vis-light, the bacteria adherence properties of the N-doped TiO<sub>2</sub> coatings on S. S and S. S substrate were tested using *Streptococcus Mutans*

strain.

Fluorescence microscope images of bacteria adherence on the S. S substrate and the N-doped TiO<sub>2</sub> coatings are shown in Fig.5(a) and Fig.5(b) respectively. The rounded region is the effective observing field of vision of the fluorescence microscope, and the small circles are the individual bacteria adherence on the specimen surfaces. Fig.6 shows the number of bacteria adherence on the S. S substrate and the N-doped TiO<sub>2</sub> coatings. Fig.5 and Fig.6 show that the bacteria adherence on the N-doped TiO<sub>2</sub> coatings is lesser than that on the S. S substrate.

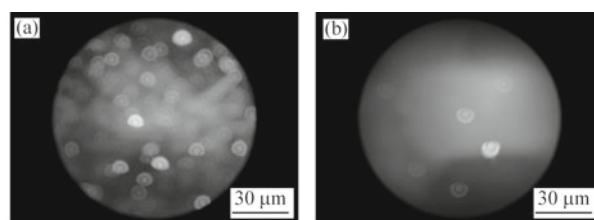


Fig.5 Fluorescence microscope images of bacterial adhesion on (a) S. S substrate and (b) N-doped TiO<sub>2</sub>

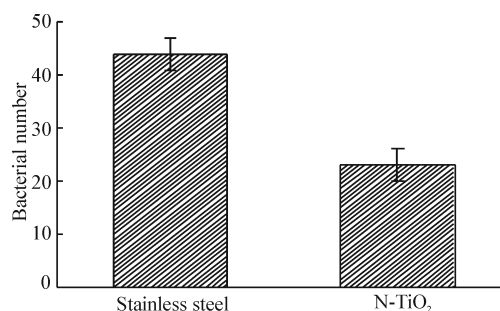


Fig.6 The number of bacterial attachment on S. S substrate and N-doped TiO<sub>2</sub>

Bacterial adherence to hard surfaces in the oral cavity is a complex of various mechanisms involving both the types of bacteria and the target surface. Non-specific interactions between the surface and the bacteria account for the initial adhesion. The affinity of bacteria to the hard surfaces is also dependent on the surface properties of the material onto which the bacteria are adsorbed. It is considered that surface roughness and surface chemical composition of the materials are the principle factors influencing bacteria adherence<sup>[12]</sup>.

Quiryren *et al*<sup>[13]</sup> considered that the total amount of adherent microorganism on the implant base had almost no distinct difference, when the surface roughness value ( $R_a$ ) of the implant base was less than  $0.2 \mu\text{m}$ . In the present study, the surface roughness values of S. S and the N-doped TiO<sub>2</sub> coated sample were less than  $0.2 \mu\text{m}$ .

The distinction in bacterial adherence among

the tested samples can be explained from two aspects as follows: (1) N-doped TiO<sub>2</sub> bactericidal activity starts its action by oxidative damage to the bacteria wall; a decrease in the interfacial energy of bacteria adhesion causes an increase in the chemical interaction between *Streptococcus Mutans* and the coatings, which is also an additional factor for the increasing anti-bacteria adherence activities. (2) Because of the positive adhesion free energy on N-doped TiO<sub>2</sub> coated sample and the negative on S. S, the negative value of the adhesion energy suggests that *Streptococcus Mutans* strain is thermodynamically favourable on the hydrophobic S. S<sup>[14]</sup>.

### 3.3 Antibacterial property

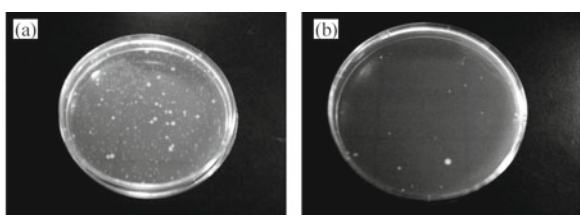


Fig.7 Photo images for the results of *S. aureus* test for (a) untreated S. S and (b) N-doped TiO<sub>2</sub> coated S. S

According to standard reduction of bacteria criterion, less than 0-20% reductions indicates no bactericidal effect; between 20-50% reduction indicates a low bactericidal effect; between 50-70% reduction indicates an expressive bactericide; greater than 70% reductions is considered a powerful bactericidal effect<sup>[15]</sup>. According to this criterion, S. S has no bactericidal effect. But, the N-TiO<sub>2</sub> coating denotes powerful bactericidal effect (Fig.7), suggesting that severe damage has occurred to the bacterium. Attack on bacteria is caused by the exposure to reactive intermediates that transferred from the surface of N-TiO<sub>2</sub> coatings to the outside of the bacteria, such as superoxide anions (O<sub>2</sub><sup>-</sup>), hydrogen peroxide (H<sub>2</sub>O<sub>2</sub>), and hydroxyl radicals (•OH), which can damage proteins, nucleic acids, etc<sup>[16]</sup>. Initial attack takes place on the cell wall, where the bactericide makes first contact with an intact bacterium<sup>[17]</sup>. Damage on cell wall will lead to the perturbation of different cellular processes, and then the leakage of the cytoplasm, finally bacteria inactivation and death<sup>[18]</sup>.

## 4 Conclusions

In summary, N-doped TiO<sub>2</sub> coatings have been successfully prepared on S. S by oxidative annealing of sputtered TiN<sub>x</sub> coatings. Thermal oxidation of TiN<sub>x</sub> coatings on S. S results in the formation of a hybrid

structure. These include a deposition layer at the surface and a gradient diffusion layer. Such a hybrid structured coatings system is proved to possess good adhesion strength with the substrate. Composition analysis shows that the coatings shield the substrates entirely. The N-doped TiO<sub>2</sub> are anatase in structure as characterized by XRD. The bacterial adherence tests demonstrated that the N-doped TiO<sub>2</sub> coatings could inhibit the *Streptococcus Mutans* adherence compared with S. S substrate. The photocatalysis and positive adhesion free energy of the N-doped TiO<sub>2</sub> coatings affects the bacterial attachment characteristics.

### References

- [1] J W Oldfield, B Todd. Technical and Economic Aspects of Stainless Steels in MSF Desalination Plants [J]. *Desalination*, 1999, 124(1-3): 75-84
- [2] R Olivares, S E Rodill, H Arzate. *In Vitro* Studies of the Biomineralization in Amorphous Carbon Films [J]. *Surf. Coat. Technol.*, 2004, 177-178: 758-764
- [3] M Fini, N N Aldini, P Torricelli, et al. A New Austenitic Stainless Steel with Negligible Nickel Content: An *in Vitro* and *in Vivo* Comparative Investigation [J]. *Biomaterials*, 2003, 24(27): 4 929-4 939
- [4] J A Disegi, L Eschbach. Stainless Steel in Bone Surgery [J]. *Injury*, 2000, 31(S4): D2-D6
- [5] T Morikawa, R Asahi, T Ohwaki, et al. Band-Gap Narrowing of Titanium Dioxide by Nitrogen Doping [J]. *Jpn. J. Appl. Phys.*, 2001, 40(6A): L561-L563
- [6] X L Cui, M Ma, W Zhang, et al. Nitrogen-Doped TiO<sub>2</sub> from TiN and Its Visible Light Photoelectrochemical Properties [J]. *Electrochem. Commun.*, 2008, 10(3): 367-371
- [7] Z Xu, B H Fang, W N Zheng, et al. A Novel Plasma Surface Metallurgy: Xu-Tec Process [J]. *Surf. Coat. Technol.*, 1990, 43-44 (P2): 1 065-1 073
- [8] X P Liu, Y Gao, Z H Li, et al. Cr-Ni-Mo-Co Surface Alloying Layer Formed by Plasma Surface Alloying in Pure Iron [J]. *Appl. Surf. Sci.*, 2006, 252(10): 3 894-3 902
- [9] F Dong, W Zhao, Z Wu. Characterization and Photocatalytic Activities of C, N and S Co-Doped TiO<sub>2</sub> with ID Nanostructure Prepared by the Nano-Confinement Effect [J]. *Nanotechnology*, 2008, 19(36): 365 607.1-365 607.10
- [10] S Sakthivel, H Kisch. Daylight Photocatalysis by Carbon-Modified Titanium Dioxide[J]. *Angew. Chem. Int. Edit.*, 2003, 42 (40): 4 908-4 911
- [11] C Gopinath. Comment on "Photoelectron Spectroscopic Investigation of Nitrogen-Doped Titania Nanoparticles" [J]. *J. Phys. Chem. B*, 2006, 110(13): 7 079-7 080
- [12] Y L Jeyachandran, S K Narayandass, D Mangalaraj, et al. A Study on Bacterial Attachment on Titanium and Hydroxyapatite Based Films [J]. *Surf. Coat. Technol.*, 2006, 201(6): 3 462-3 474
- [13] M Quirynen, H C Van der Mei, C M L Bollen, et al. Clinical Relevance of the Influence of Surface Free Energy and Roughness on the Supragingival and Subgingival Plaque Formation in Man [J]. *Colloid Surf. B: Biointerf.*, 1994, 2(1-3): 25-31
- [14] W Y Su, S C Wang, L Wu, et al. Surface Anti-Bacterial Adhesion Characteristics of TiO<sub>2</sub>-Coated PMMA [J]. *J. Struct. Chem.*, 2009, 11(28): 1 497-1 502
- [15] H Y Lee, Y H Park, K H Ko. Correlation between Surface Morphology and Hydrophilic/Hydrophobic Conversion of MOCVD TiO<sub>2</sub> Films [J]. *Langmuir*, 2000, 16(18): 7 289-7 293
- [16] Z Huang, P C Maness, D M Blake, et al. Bactericidal Mode of Titanium Dioxide Photocatalysis [J]. *J. Photochem. Photobiol. A. Chem.*, 2000, 130(2-3): 163-170
- [17] B Halliwell, J M C Gutteridge. *Free Radicals in Biology and Medicine*[M]. New York: Oxford University Press, 1989
- [18] J Lonnen, S Kilvington, S C Kehoe, et al. Solar and Photocatalytic Disinfection of Protozoan, Fungal and Bacterial Microbes in Drinking Water [J]. *Water Res.*, 2005, 39(5): 877-883